*Essential Readings in Light Metals: Aluminum Reduction Technology.*
Edited by Geoff Bearne, Marc Dupuis and Gary Tarcy.



# MODELING THE BUBBLE DRIVEN FLOW IN THE ELECTROLYTE AS A TOOL FOR SLOTTED ANODE DESIGN IMPROVEMENT

Dagoberto S. Severo[1], Vanderlei Gusberti[1], Elton C. V. Pinto[1], Ronaldo R. Moura[2].

[1] PCE Engenharia S/S Ltda, Rua Caete, 162 - Porto Alegre RS - Brazil
[2] ALBRAS - Alumínio Brasileiro S.A., Estrada PA 483 Km 21, Vila Murucupí , Barcarena PA - Brazil

Keywords: Slotted anode, Gas bubbles, Multiphase flow, Numerical simulation

**Abstract**

Slotted anodes have been used in recent years by aluminum smelters in order to reduce gas bubble resistance at the anode/electrolyte interface. Bubbles are responsible also for part of the cell electric noise. The main objective of this study is to present a CFD model of the bubble driven flow in the electrolyte. The model is detailed enough to differentiate the effects of different anode and slot geometries. We consider the multiphase flow as a continuous liquid/dispersed gas pair, turbulent and steady state. A comparison with measurements found in the literature is made. The model is applied to study options for the slotted anodes at ALBRAS. The simulations were done using the commercial code ANSYS CFX 10.0.

## Introduction

Nowadays, most of the aluminum smelters are seeking ways to increase the current and reduce energy consumption. The anodic gas bubbles in the Hall-Héroult cell are a very important player in this process.

The gas (mainly carbon dioxide) creates a layer below the anode surface. This layer contributes to the bath flow that is responsible for the alumina dissolution and its transport into the interpolar space. However, the bubble layer increases the voltage drop and electric noise (voltage fluctuation) of the cell. The bubble voltage could be as high as 300 mV [1] depending on the anode current density and alumina concentration. Also, the gas induces bath flow and bath turbulence, which influence the current efficiency [4].

The direct measurement of the bubble layer is not possible due the harsh environment - high temperature and corrosiveness of the bath. Physical models have been used to study the phenomenon [6,8]. There are some studies that have been made by numerical modeling where only gas driven flow has been considered [10,11]. To the best of author's knowledge, there is only one paper that shows modeling of MHD and gas driven flow coupled [5].

It is well known that slots in the anodes are effective in reducing the voltage drop and noise due to bubbles [2,3]. This happens because the slots allow a better elimination of the gas from the anode bottom surface. Improvements in current efficiency are expected too.

There are a few physical models of slotted anodes [6,9] but numerical modeling is scarce in the literature [7]. Until now slot design has been done empirically, taking into account the anode forming process. Depending on the extrusion direction, the anode slots can be made longitudinal or transversal.

The main objective of this work was to analyze the slots used by ALBRAS and to find a slot efficiency criterion using CFD tools. Different anode and slot geometries were analyzed.

## Model description

The commercial CFD software package ANSYS CFX solves the hydrodynamics equations (Navier-Stokes and mass conservation) by Finite Volume Method. This software has several options for multiphase inhomogeneous flow. We chose the VOF (Volume of Fluid) Method with a pair of continuous/disperse fluids. Turbulence was solved using the traditional k-ε model for the continuous phases, and Dispersed Phase Zero-Equation model for the bubbles. The inter-phase momentum transfer model used was Ishii Zuber. Sato Enhanced Eddy Viscosity was used for turbulence transfer between the phases. All models used are fully detailed in literature [13].

Validation Model:

Published experimental data, obtained on a physical model were used for the validation of our mathematical model [6]. Continuous phase is w*ater* and the dispersed phase is *air* (mean bubble diameter of 20 mm). The gas generation at the source (anode bottom) is at a rate of 103 L/min of air (with slot) and 120 L/min of air (without slot). The model is isothermal at 25°C. The finite volume model was built to represent the bath around three anodes (Figure 1) according to the geometry used for PIV measurements in the physical model published. Like the original study, our mathematical model compared the flow with and without a longitudinal slot at the central anode; both cases with inter-anode gap of 20 mm. Gas outflow occurs at the top of the model (degassing boundary). Smooth non-slippery walls enclose the domain.

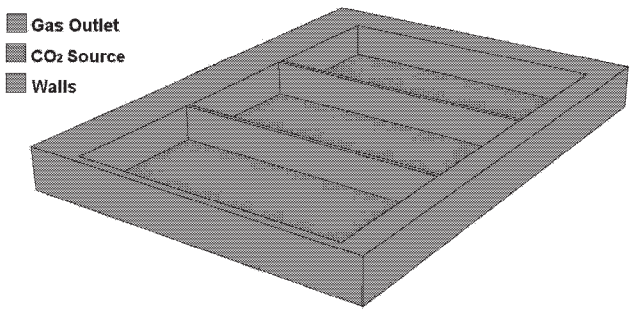


Figure 1. Three anode model (without slot) for model validation with previously published experimental data.

Application Models:
Continuous phase is *Bath* and the disperse phase is $CO_2$ (mean bubble diameter of 5 mm). The models are isothermal at 960°C. The rate of $CO_2$ generation of 9,854e-4 kg/m²s at the source was obtained by a known formula [4], and it corresponds to a cell working at 178 kA with current density of 0.85 A/cm² at the anodes. As in the previous model, the gas outflow occurs at the top of the domain (degassing boundary). The modeled geometry of the anode was the one used by ALBRAS.

A single anode was tested without a slot, with two transversal and with two longitudinal slots. For these tests only the bubble driven flow was considered. A comparison of the effectiveness of the bubble extraction was made by taking the volume of $CO_2$ under the anode after the steady state flow was achieved. Symmetries for all variables were used at the inter-anode and central channels (Figure 2). Two types of slots were tested – one considering the slot fully immersed in the bath and other where the slot is half immersed in order to simulate the condition in the beginning of the anode life.

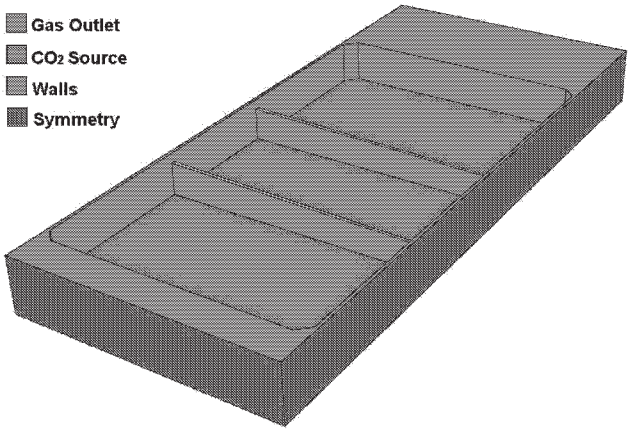


Figure 2. Single anode model, tested with two transversal, two longitudinal, and with no slots.

A full pot model was also made, in which the bath flow was modeled with all the anodes. The bubble driven flow alone, without slots, was calculated. The influence of the metal flow and of the MHD-induced bath flow was also tested. In the coupled model, both transversal and longitudinal slots were included. The carbon consumption leads to a given distribution of anode slot heights (taking into account the changing sequence): some slots are half immersed (on new anodes), some are fully immersed and some anodes are without slots (old anodes).

As previously the degassing boundary was at the top of the domain, the gas source at the bottom of the anodes, and walls represented the surrounding ledge. The metal drag on the bath was taken into account by representing the metal velocity as a moving wall boundary condition at the interface of the liquids at the bottom of the model (Figure 3). The metal velocity at the interface (Figure 4) and the MHD forces in the bath were obtained by previous modeling [12].

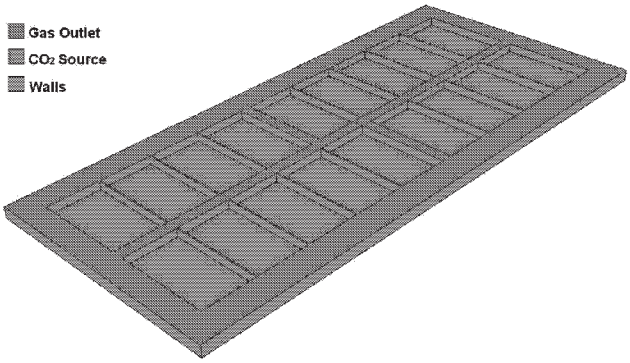


Figure 3. Boundaries and body forces of the full-pot model.

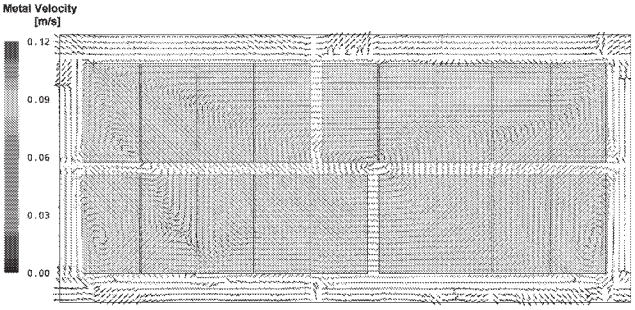


Figure 4. Metal velocity at the bath-metal interface for the full-pot model.

**Results**

Validation Model:
Figures 5 and 6 show the mathematical model results in the center channel for both models – with and without the slot. Vectors show water phase velocity and contours show air velocity.
When comparing the calculations with PIV measurements one can see the same effect that the slot moves the recirculation zone down and to the right. The center of the recirculation in the case of no slot is located at y/H = 0.68 in terms of relative vertical distance from the base of the model. In case of the slot presence it is located at y/H = 0.35. PIV measurements showed 0.66 and 0.37 respectively.

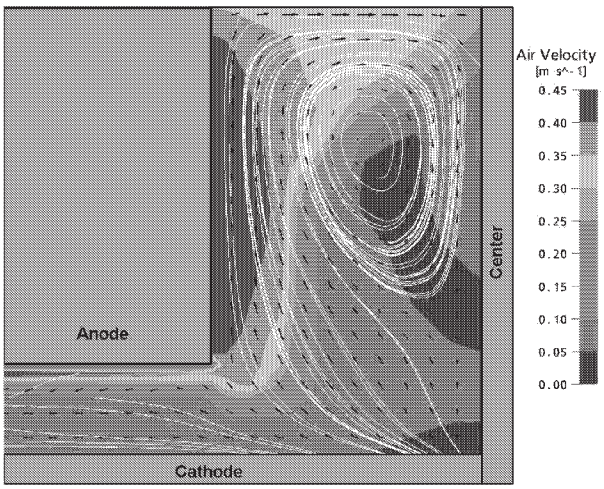


Figure 5. CFD results in the center channel mid-point of the anode for the anode without slot.

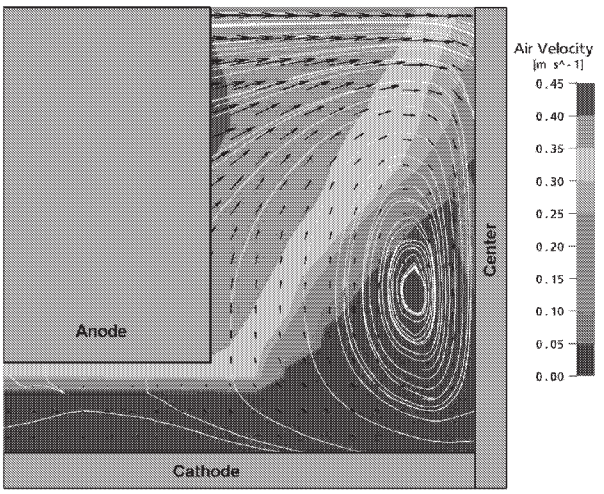


Figure 6. CFD results in the center channel mid-point of the anode for the anode with slot.

Single Anode Model

Figures 7, 8 and 9 show the mathematical model results for bath phase velocity in 3D vectors for the region close to the center channel.

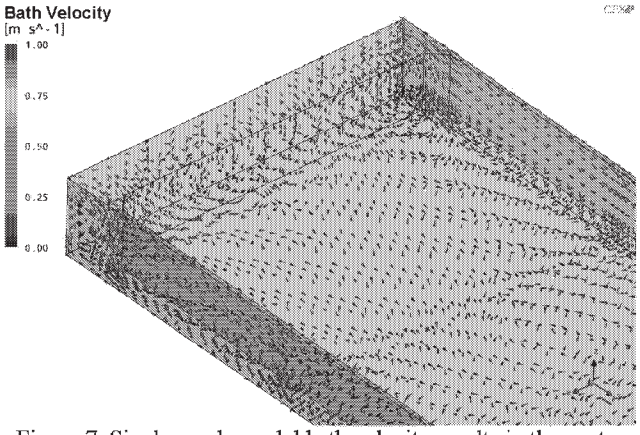


Figure 7. Single anode model bath velocity results in the center channel for the anode without slot.

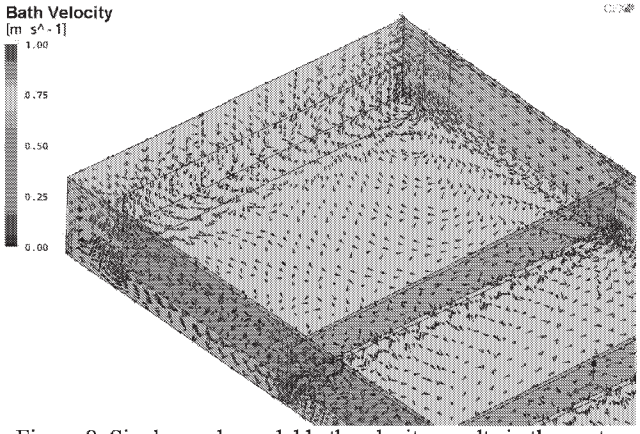


Figure 8. Single anode model bath velocity results in the center channel for the anode with transversal slot.

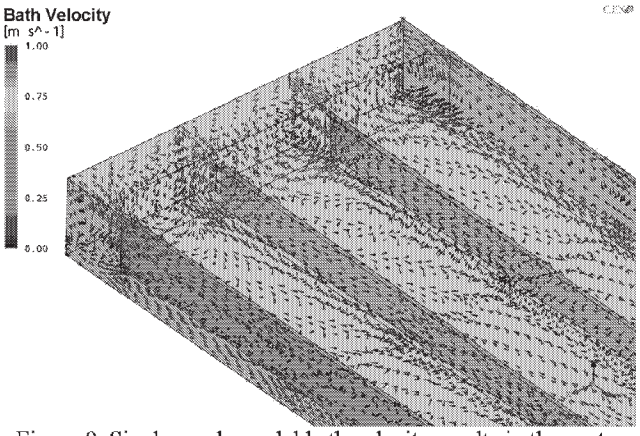


Figure 9. Single anode model bath velocity results in the center channel for the anode with longitudinal slot.

We can see almost no difference in the bath velocity at mid-point of the anode - between the model without slot and the one with the transversal slot. However, in case of the longitudinal slot there is some increase in the bath velocity at that location. There is a great increase in the bath velocity in the space between anodes with transversal slots included.

Full Pot Model

Figures 10, 11, 12 and 13 show the bath flow for the full pot model in the middle of the interpolar distance. Figure 14 shows the bath velocity for a section in the center channel.

Table I shows a compilation of the results for the volume below the anode bottom surface where k is the turbulent kinetic energy.

Table I. Results below the anode bottom surface

| | Gas volume (L) | Bath average velocity (cm/s) | Bath average k ($10^{-3}$ $m^2/s^2$) |
|---|---|---|---|
| **Single anode model** | | | |
| Without slot | 5.842 | 6.4 | 3.00 |
| Transversal slot (fully immersed) | 3.797 | 5.7 | 1.57 |
| Transversal slot (half immersed) | 3.770 | 5.7 | 1.57 |
| Longitudinal slot (fully immersed) | 3.201 | 6.7 | 1.71 |
| Longitudinal slot (half immersed) | 3.060 | 4.9 | 1.65 |
| **Full pot model** | | | |
| Without MHD and without slot | 5.803 | 8.9 | 2.68 |
| With MHD and without slot | 5.895 | 11.2 | 2.36 |
| With MHD and transversal slot | 4.876 | 10.1 | 1.85 |
| With MHD and longitudinal slot | 4.514 | 9.7 | 1.57 |

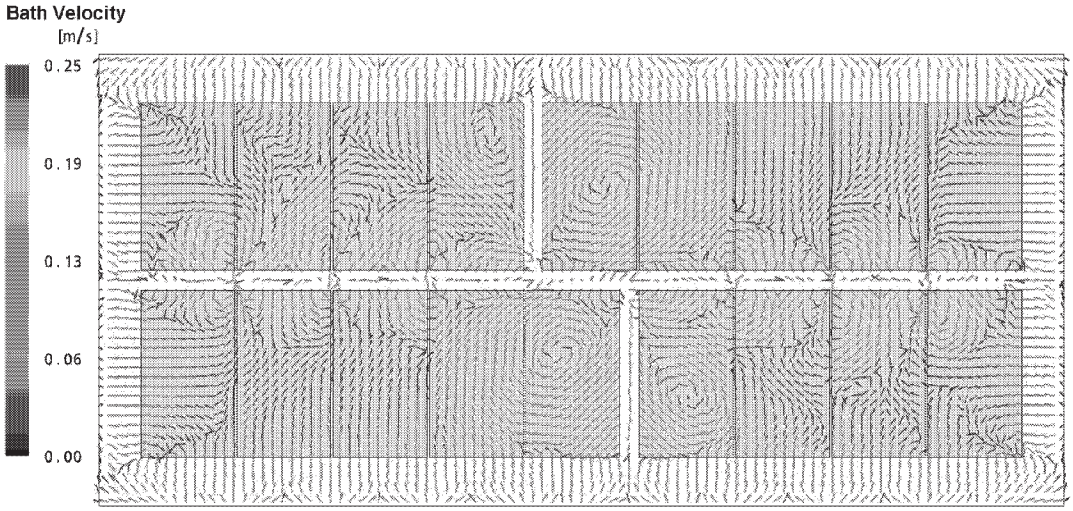


Figure 10. Full pot model bath velocity without MHD without slots

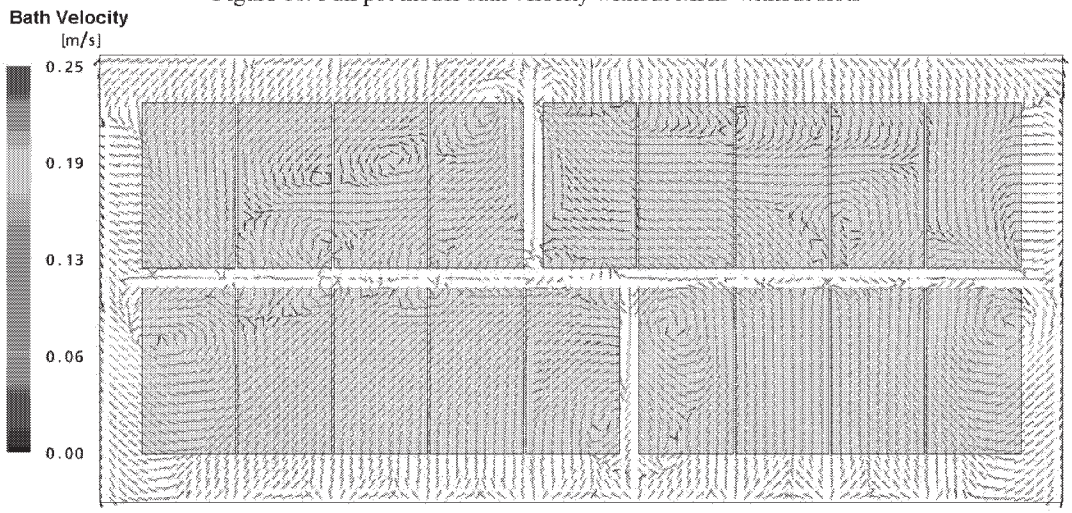


Figure 11. Full pot model bath velocity with MHD without slots

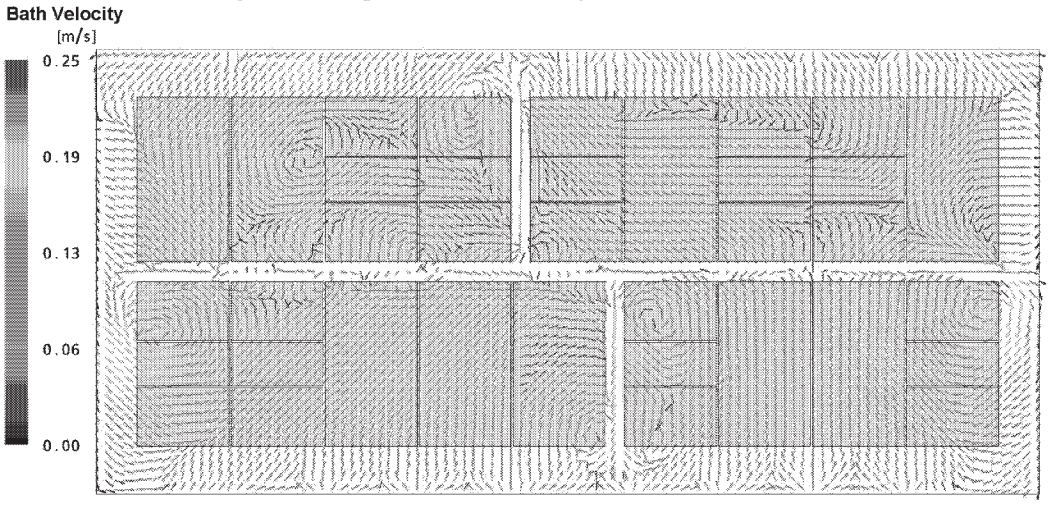


Figure 12. Full pot model bath velocity with MHD for transversal slots

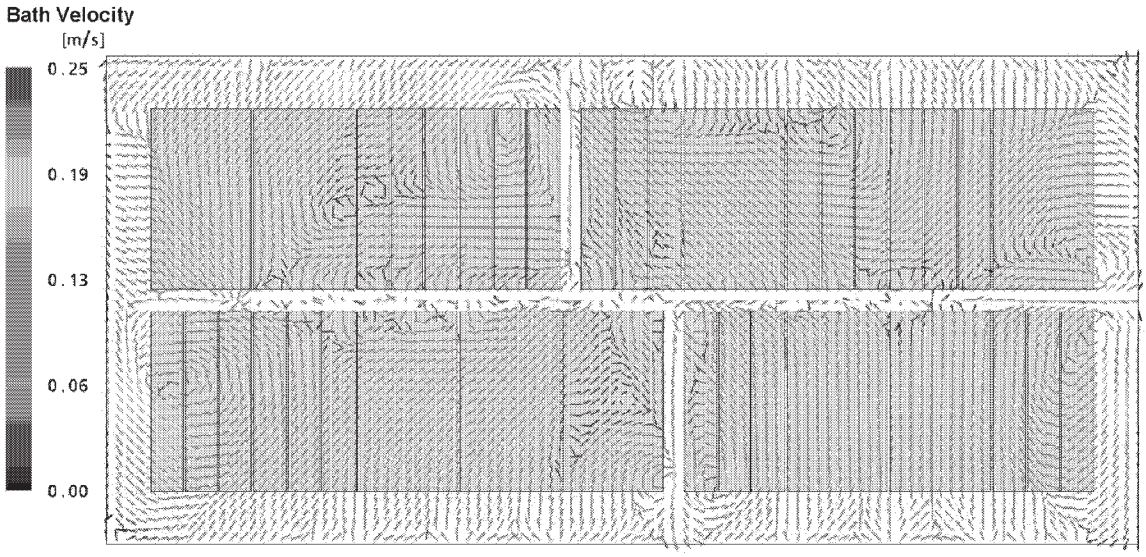


Figure 13. Full pot model bath velocity with MHD for longitudinal slots

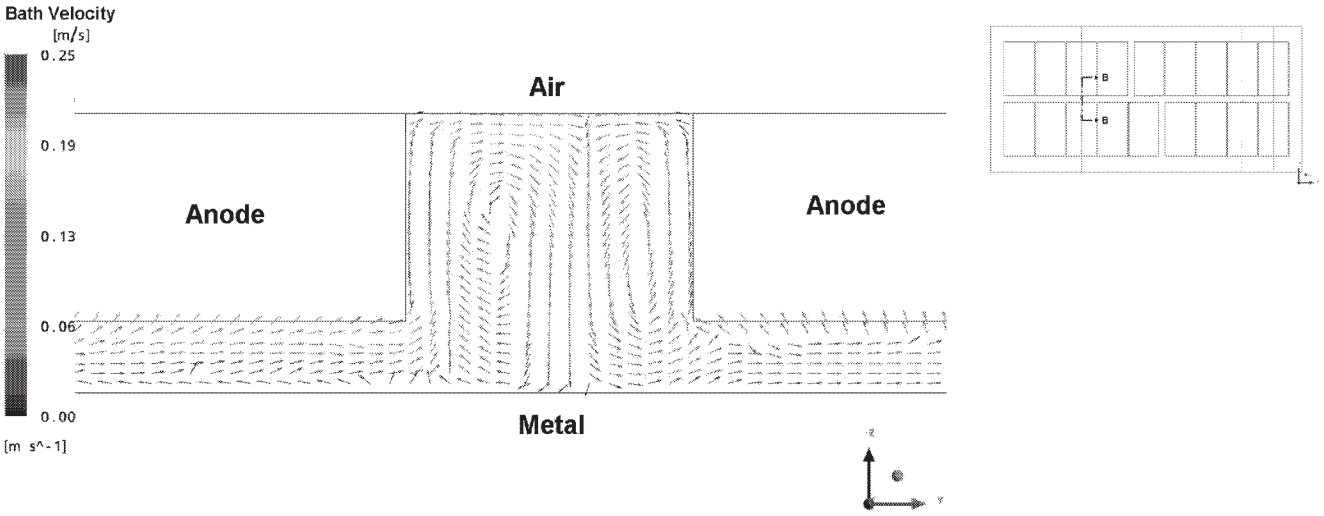


Figure 14. Full pot model bath velocity with MHD without slots – Section in the center channel

## Discussion

The decrease in pot resistance in the case of transverse slots observed by ALBRAS of 0.10 μΩ and noise by 0.04 μΩ could be explained by the decrease in the volume of gas below the anode by 17% from 5.895 L to 4.876 L. The difference between transversal and longitudinal slots is only 7% in the volume of gas below the anode and this could explain why ALBRAS did not observe significant differences between them during the tests.

As can be seen in Table I, the gas volume below the anodes is underestimated in the single anode model because it is not possible to take into account the anode consumption that reduces the number of slotted anodes in the pot.

The difference between the slot fully or only half immersed is that there is less gas below the anode for the half immersed slot. This difference is small for the transversal slots. However, for the longitudinal the difference is bigger and there is a significant reduction in the average bath velocity and turbulent kinetic energy when the slot is half immersed. This is because the path to be covered by the gas is bigger for the longitudinal slots when fully immersed.

Convective transport is related to average bath velocities. The turbulent kinetic energy (k) distribution gives an indication of the intensity of local mixing. Both are related to alumina dissolution and current efficiency.

The full model allows analyzing the MHD influence. We can see that the MHD increases the average bath velocity and decreases the turbulent kinetic energy (Table I).

The effect of the transversal and longitudinal slots is to reduce the average bath velocity and the turbulent kinetic energy for the volume bellow the anode bottom. This effect is beneficial for the

region below the anode because it will reduce the reoxidation of the metal dissolved in the electrolyte [5].

When comparing transversal and longitudinal slots we can see that the average bath velocity and turbulence underneath the anodes decreases for longitudinal slots. This could explain why longitudinal slots are believed to be better in terms of current efficiency than transversal slots.

## Conclusions

A CFD model of the bubble driven flow in the electrolyte was presented. The model is detailed enough to differentiate the effects of different anode and slot geometries. A full pot model, with MHD and bubble driven flow coupled, is necessary in order to observe all the significant phenomena that occur.

The full pot model needs validation that could be done using the technique presented by Kobbeltvedt [14].

The results show that the effect of the slots on the bath flow is very complex and time dependent due the different slots that exist in a pot at the same time. The complexity is a function of anode change sequence as well as the carbon consumption.

We can conclude that the simulation is a useful tool to anode slot design. The model with MHD and bubble driven flow coupled could be used to study the point feeder operation. This will be next step in our study.

## Acknowledgement

The authors wish to thank Mr. Vinko Potocnik for his critical and careful review of the manuscript.

## References

1. N. Richards et al., “Characterization of the Fluctuation in Anode Current Density and Bubble Events in Industrial Reduction Cells”, *Light Metals*, (2003), 315-322.
2. H.P. Dias and R.R. de Moura, “The Use of Transversal Slot Anodes at Albras Smelter”, *Light Metals*, (2005), 341-344.
3. S.C. Tandon and R.N. Prasad, “Energy Saving in Hindalco´s Aluminium Smelter”, *Light Metals*, (2005), 303-309.
4. T. Haarberg, A. Solheim and S.T. Johansen "Effect of anodic gas release on current efficiency in Hall-Héroult cells" *Light Metals,* (1998), 475-481.
5. M.M. Bilek, W.D. Zhang and F.J. Stevens, “Modelling of Electrolyte Flow and Its Related Transport Processes in Aluminium Reduction Cells" Light *Metals,* (1994), 323-331.
6. M.A. Cooksey and W. Yang, "PIV Measurements on Physical Models of Aluminium Reduction Cells", *Light Metals*, (2006), 359-365.
7. L.I. Kiss, S. Poncsak and J. Antille, "Simulation of the Bubble Layer in the Aluminum Electrolysis Cells", *Light Metals*, (2005), 559-564.
8. D.C. Chesonis and A.F. LaCamera, "Influence of Gas - Driven Circulation on Alumina Distribution and Interface Motion in a Hall-Héroult Cell", *Light Metals* (1990), 211-220.
9. J.J.J. Chen, K.X. Qian and J.C. Zhao, "Resistance Due to the Presence of Bubbles in an Electrolytic Cell with a Grooved Anode", *Chemical Engineering Research & Design*, 79(A4), (2001), 383-388.
10. L.I. Kiss, S. Poncsák and J. Antille, “Simulation on the bubble layer in aluminum electrolysis cells,” *Light Metals* (2005), 559-564.
11. K. Bech, S. T. Johansen, A. Solheim and T. Haarberg, “Coupled current distribution and convection simulator for electrolysis cells,” *Light Metals* (2001), 463-468.
12. D. S. Severo, A. F. Schneider, E. C. V. Pinto, V. Gusberti, V. Potocnik, “Modeling Magnetohydrodynamics of Aluminum Electrolysis Cells with ANSYS and CFX”, *Light Metals*, (2005), 475-480.
13. CFX 10 User Manual - Solver Modelling, Multiphase Flow Modelling.
14. O. Kobbeltvedt and B.P. Moxnes, “On the Bath Flow, Alumina Distribution and Anode Gas Release in Aluminium Cells”, *Light Metals* (1997), 369-376.